

## Fourth-Order Electrodynamic Corrections to the Lamb Shift\*

Thomas Appelquist and Stanley J. Brodsky†

Stanford Linear Accelerator Center, Stanford University, Stanford, California 94305

(Received 30 April 1970)

The fourth-order radiative correction to the slope at  $q^2=0$  of the Dirac form factor of the free-electron vertex is calculated using computer techniques. The result  $m^2 \partial F_1^{(4)}(0)/\partial q^2 = (\alpha/\pi)^2 (0.48 \pm 0.07)$  disagrees with previous calculations and implies a new theoretical value for the order  $\alpha^2 (Z\alpha)^4 mc^2$  contribution to the Lamb shift. The new values for the  $2S_{1/2} - 2P_{1/2}$  separation in H and D are increased by  $0.35 \pm 0.07$  MHz and are in good agreement with the results of recent experiments.

### I. INTRODUCTION

The calculations and measurements of the Lamb shift have had a profound influence on the development of quantum electrodynamics (QED). The first measurements of the  $2S_{1/2}$ -level displacement from the  $2P_{1/2}$  level in hydrogen by Lamb and Retherford<sup>1</sup> stimulated the concept of mass renormalization and led Bethe<sup>2</sup> to carry out the first finite calculation of the self-interaction of the electron with the quantized electromagnetic field. The relativistic theory that emerged has met all of its experimental challenges with great quantitative success<sup>3</sup>; the agreement is better than 10 ppm for the hyperfine splitting of hydrogen and muonium and better than 0.1 ppm in the total magnetic moments of the electron and muon.

Ironically, the only tests of QED which show a serious disagreement ( $\approx 200 \pm 70$  ppm) between theory and experiment are the  $2S_{1/2} - 2P_{1/2}$  separations in hydrogen and deuterium. The disagreement has become more acute with recent measurements by Robiscoe and Cosens<sup>4</sup> and others<sup>5</sup> of the Lamb interval in H, D, He\*, Li\*\*, and three measurements<sup>6</sup> of the  $2P_{3/2} - 2S_{1/2}$  interval in H. The latest experimental results are shown in Table I. The theoretical predictions have become more precise over the years with the development of new calculational techniques by Layzer,<sup>7</sup> Karplus, Klein, and Schwinger,<sup>8</sup> and Erickson and Yennie<sup>9</sup> for the evaluation of the order- $\alpha$  (second order in perturbation theory) self-energy expression for the Coulomb-bound electron. In addition, the nuclear recoil corrections ( $m/M$  contributions beyond reduced-mass effects) originally evaluated by Salpeter<sup>10</sup> from the Bethe-Salpeter equation have now been checked by Grotch and Yennie<sup>11</sup> using an effective potential technique. The various contributions to the theoretical prediction of the  $2S_{1/2} - 2P_{1/2}$  separation in H are shown in column 1 of Table II. The total result  $1057.56 \pm 0.09$  MHz ("limit of error") is in clear disagreement with the experimental numbers in Table I. The corresponding result for D,  $1058.82 \pm 0.15$  MHz is in similar disagreement. The only

experimentally relevant contribution in the table, not checked by independent methods, is the fourth-order electron self-energy correction proportional to the slope of the Dirac form factor at  $q^2 = 0$ , labeled  $F_1'(0)$ . This contribution was first estimated by Weneser, Bersohn, and Kroll<sup>12</sup> and calculated completely analytically by Soto.<sup>12</sup>

In this paper we present the details of a new calculation<sup>13</sup> of this fourth-order [ $\alpha^2(Z\alpha)^4 m$ ] radiative contribution to the Lamb shift. Our result differs from the previous calculation of Soto<sup>12</sup> and, when added to the other contributions of Table II, leads to new theoretical values for the Lamb shift in H and D of  $1057.91 \pm 0.16$  and  $1059.17 \pm 0.22$  MHz, respectively, an increase of  $0.35 \pm 0.07$  MHz over the previous compilation of Taylor *et al.*<sup>4</sup> A tabulation of the various contributions to the theoretical result for H, including the revised fourth-order contribution of  $F_1'(0)$ , is given in Table II. The comparison of the revised theory with experiment is given in the last column of Table I. The majority of the experimental results are within one standard deviation of theory, leaving only one high-precision measurement<sup>5</sup> which uses the nonatomic beam "bottle" method, in serious disagreement. The one-standard-deviation error limits used in the comparison of theory and experiment were computed by combining the standard-deviation experimental error assigned by Taylor *et al.*<sup>4</sup> with one-third of the limit of error (LE) of the theoretical result.

### II. DESCRIPTION OF CALCULATION

In principle, one must compute radiative corrections to atomic energy levels using bound-state perturbation theory. Instead, for the terms of interest here, the  $\alpha^2(Z\alpha)^4 m$  contribution, we can use the so-called scattering approximation<sup>12,14</sup> which is calculational simpler. In this approach, one calculates the radiative corrections to the scattering of a free electron and then infers from this a modified interaction potential from which the level shifts can be calculated.

The matrix element of the electromagnetic current between two free-electron states is given by<sup>15</sup>

$$-ie\bar{u}(p + \frac{1}{2}q)\{\gamma_\mu F_1(q^2) + (1/4m) \times [q', \gamma_\mu] F_2(q^2)\}u(p - \frac{1}{2}q). \quad (2.1)$$

$$\Delta E(n, j, l) = \delta_{l0} \frac{4(Z\alpha)^4 mc^2}{n^3} m^2 \frac{\partial F_1(q^2)}{\partial q^2} \Big|_{q^2=0}, \quad (2.2)$$

The modification of the Coulomb interaction due to  $F_1(q^2)$  implies an energy shift,<sup>9</sup>

plus contributions of higher order in the binding parameter  $Z\alpha$ . In second order,

TABLE I. Lamb shift in hydrogenic atoms (in MHz).

Atom	Ref.	$\mathcal{L}_{\text{expt}}^{\pm} (\pm 1\sigma)^a$	(Old) theory <sup>b</sup> ( $\pm$ LE)	(Old) expt-theory ( $\pm 1\sigma$ )	Revised theory <sup>c</sup> ( $\pm$ LE)	Revised expt-theory ( $\pm 1\sigma$ )
(a) Lamb shift in H and D						
H ( $n=2$ ) <sup>d</sup>			1057.56 $\pm$ 0.09		1057.91 $\pm$ 0.16	
	e	1057.77 $\pm$ 0.06		0.21 $\pm$ 0.07		-0.14 $\pm$ 0.08
	f	1057.90 $\pm$ 0.06		0.34 $\pm$ 0.07		-0.01 $\pm$ 0.08
	g	(1057.65 $\pm$ 0.05)		0.09 $\pm$ 0.06		-0.26 $\pm$ 0.07
	h	(1057.78 $\pm$ 0.07)		0.22 $\pm$ 0.08		-0.13 $\pm$ 0.09
	i	(1057.86 $\pm$ 0.06)		0.30 $\pm$ 0.07		-0.05 $\pm$ 0.08
D ( $n=2$ ) <sup>a</sup>			1058.82 $\pm$ 0.15		1059.17 $\pm$ 0.22	
	j	1059.00 $\pm$ 0.06		0.18 $\pm$ 0.08		-0.17 $\pm$ 0.09
	k	1059.28 $\pm$ 0.06		0.46 $\pm$ 0.08		+0.11 $\pm$ 0.09
(b) Lamb shift in other atoms						
He* ( $n=2$ )			14038.9 $\pm$ 4.1		14044.5 $\pm$ 5.2	
	l	14040.2 $\pm$ 1.8		1.3 $\pm$ 2.2		-4.3 $\pm$ 2.5
	m	14045.4 $\pm$ 1.2		6.5 $\pm$ 1.8		1.0 $\pm$ 2.1
He* ( $n=3$ )			4182.7 $\pm$ 1.2		4184.4 $\pm$ 1.5	
	n, o	4182.0 $\pm$ 1.0		-0.3 $\pm$ 1.1		-2.0 $\pm$ 1.1
	p	(4184.0 $\pm$ 0.6)		1.3 $\pm$ 0.7		-0.4 $\pm$ 0.8
He* ( $n=4$ )			1768.3 $\pm$ 0.5		1769.0 $\pm$ 0.6	
	q	1776.0 $\pm$ 7.5		-2.3 $\pm$ 7.5		-3.0 $\pm$ 7.5
	r, o	1768.0 $\pm$ 5.0		-0.3 $\pm$ 5.0		-1.0 $\pm$ 5.0
	s	(1769.4 $\pm$ 1.2)		+1.1 $\pm$ 1.3		0.4 $\pm$ 1.3
Li** ( $n=2$ )			6273.0 $\pm$ 45.0		62771.0 $\pm$ 50.0	
	t	63031.0 $\pm$ 327.0		288.0 $\pm$ 333.0		260.0 $\pm$ 333.0

<sup>a</sup>The values for  $\mathcal{L}_{\text{expt}}$  listed in parenthesis are computed from experimental measurements of the large interval  $\Delta E - \mathcal{L} = \Delta E (2P_{312} - 2S_{1/2})$  and the theoretical fine structure (See Table III).

<sup>b</sup>B. N. Taylor *et al.*, Ref. 4.

<sup>c</sup>Corresponds to corrected result for the fourth-order contributions discussed in this paper. We use conventions of B. N. Taylor *et al.*, Ref. 4, and the limit of error (LE) is three standard deviations.

<sup>d</sup>The experimental results for H and D are from Refs. 1-3.

<sup>e</sup>Reference 1(b).

<sup>f</sup>Robiscoe (unpublished). This includes a correction for the non-Maxwellian velocity distribution of the atoms in the beam [Ref. 4(a); see note added in proof of Ref. 4(b)].

<sup>g</sup>Reference 6(a).  $(\Delta E - \mathcal{L})_{\text{expt}} = 9911.38 \pm 0.03$ .

<sup>h</sup>Reference 6(b).  $(\Delta E - \mathcal{L})_{\text{expt}} = 9911.25 \pm 0.06$ .

<sup>i</sup>Reference 6(c).  $(\Delta E - \mathcal{L})_{\text{expt}} = 9911.17 \pm 0.04$ .

<sup>j</sup>Reference 1(b).

<sup>k</sup>B. L. Cosens (unpublished). This includes a correction for the non-Maxwellian velocity distribution of the atoms in the beam [Ref. 4(a); see note added in proof of Ref. 4(b)].

<sup>l</sup>E. Lipworth and R. Novick, Phys. Rev. **108**, 1434 (1957).

<sup>m</sup>M. A. Narasimham, Ph.D. thesis, University of Colorado, 1968 (unpublished).

<sup>n</sup>D. Mader and M. Leventhal, International Conference on Atomic Physics, New York University, 1968 (unpublished).

<sup>o</sup>B. N. Taylor, W. H. Parker, and D. N. Langenberg, Rev. Mod. Phys. **41**, 375 (1969).

<sup>p</sup>Ref. o;  $\Delta E - \mathcal{L} = 47843.8 \pm 0.5$

<sup>q</sup>L. L. Hatfield and R. N. Hughes, Phys. Rev. **156**, 102 (1967).

<sup>r</sup>R. R. Jacobs, K. R. Lea, and W. E. Lamb, Jr., Bull. Am. Phys. Soc. **14**, 525 (1969).

<sup>s</sup>Ref. o;  $\Delta E - \mathcal{L} = 20179.7 \pm 1.2$ .

<sup>t</sup>C. Y. Fan, M. Garcia-Munoz and I. A. Sellin, Phys. Rev. **161**, 6 (1967).

TABLE II. Tabulation of the theoretical contributions to the Lamb interval  $\mathcal{L} = \Delta E(2S_{1/2} - 2P_{1/2})$  in H.<sup>a</sup>

Description	Order	Old tabulation	New tabulation
2nd-order self-energy	$\alpha(Z\alpha)^4 m (\ln Z\alpha, 1)$	1 079.32 ± 0.02	1 079.32 ± 0.02
2nd-order vacuum polarization	$\alpha(Z\alpha)^4 m$	- 27.13	- 27.13
2nd-order remainder	$\alpha(Z\alpha)^5 m$	7.14	7.14
	$\alpha(Z\alpha)^6 m (\ln^2 Z\alpha, \ln Z\alpha, 1)$	- 0.38 ± 0.04	- 0.38 ± 0.04
4th-order self-energy	$\alpha^2(Z\alpha)^4 m F_1'(0)$	0.10 ±	0.45 ± 0.07
	$F_2(0)$	- 0.10	- 0.10
	$\alpha^2(Z\alpha)^5 m$	± 0.02	± 0.02
4th-order vacuum polarization	$\alpha^2(Z\alpha)^4 m$	- 0.24	- 0.24
Reduced-mass corrections	$\alpha(Z\alpha)(m/M)m \{\ln Z\alpha, 1\}$	- 1.64	- 1.64
Recoil	$(Z\alpha)^5(m/M)m \{\ln Z\alpha, 1\}$	0.36 ± 0.01	0.36 ± 0.01
Proton size	$(Z\alpha)^4(mR_p)^2 m$	0.13	0.13
	$\mathcal{L} = \Delta E(2S_{1/2} - 2P_{1/2})$	1 057.56 ± 0.08	1 057.91 ± 0.16 (L. E.)
$\alpha^{-1} = 137.036 08$	$\Delta E(2P_{3/2} - 2S_{1/2})$	9 911.47 ± 0.15	9 911.12 ± 0.22 (L. E.)
	$\Delta E(2P_{3/2} - 2P_{1/2})$	10 969.03 ± 0.12	10 969.03 ± 0.12 (L. E.)

<sup>a</sup>References to the various entries may be found in G. W. Erickson and D. R. Yennie (Ref. 9) and B. N. Taylor *et al.* (Ref. 4). The dependence on nuclear charge is retained to distinguish binding and radiative corrections. Column 1 gives the former theoretical result which includes the order- $\alpha^2(Z\alpha)^4 m$  contribution to the energy shift from the slope of the Dirac form factor in fourth order as given by M. Soto (Ref. 12). The revised theory, corresponding to the corrected value for this contribution as given by Eqs. (2.5) and (2.2), is listed in column 2. Note that fourth-order contributions to the Lamb interval also arise from the fourth-order anomalous moment and vacuum-polarization corrections.

$$m^2 \frac{\partial F_1^{(2)}(q^2)}{\partial q^2} \Big|_{q^2=0} = \frac{\alpha}{3\pi} \left[ \ln \left( \frac{m}{\lambda} \right) - \frac{3}{8} \right] \quad (\lambda \ll m) \quad (2.3)$$

is infrared divergent for a free electron. This divergence reflects the fact that the scattering approximation is invalid for the order- $\alpha$  contribution. In the correct bound-state treatment of the low-frequency region, the photon mass  $\lambda$  is replaced by an appropriate energy difference, the Bethe energy  $|E_n - E_m|_{av}$ , and Eq. (2.2) with (2.3) gives the dominant contribution to the Lamb shift. Photons of wavelengths much larger than atomic dimensions do not contribute to the energy shift, since they contribute equally to the self-energy of free and bound electrons.

The order- $\alpha^2$  contribution to the slope of the Dirac form factor was first shown to be convergent in the infrared by Weneser, Bersohn, and Kroll (WKB).<sup>12,16</sup> This result was verified by Mills and Kroll<sup>14</sup> starting from the fourth-order self-energy expression for the energy shift of the bound electron. These authors have also given an explicit proof that the scattering approximation is correct in fourth order. Soto<sup>12</sup> was able to perform the required integrals analytically (including those only bounded by WKB) and found some small errors in WBK's work. His result was

$$m^2 \frac{\partial F_1^{(4)}}{\partial q^2} \Big|_{q^2=0} = \frac{\alpha^2}{\pi^2} [0.1076\dots], \quad (2.4)$$

which yields the contribution 0.102 MHz to the  $2S_{1/2} - 2P_{1/2}$  separation in H and D. Other fourth-order

contributions to the Lamb shift from  $F_2(0)$  and vacuum polarization corrections are included in the tabulation of Table II. Contributions of order  $q^4$  from  $F_1(q^2)$  and vertex-vacuum polarization cross terms yield corrections one order of  $Z\alpha$  smaller.

The Feynman diagrams which are required to calculate the fourth-order contribution to the slope  $F_1'(0)$  are shown in Fig. 1. The calculational and renormalization techniques are similar to those used in the magnetic-moment  $F_2(0)$  calculations of Karplus and Kroll<sup>17</sup> and Petermann,<sup>18</sup> although the slope calculation involves more complicated numerator structures and contributions from differentiation of denominators with respect to  $q^2$ . Furthermore, in the standard gauge, individual graphs have  $\ln^2 \lambda$  and  $\ln \lambda$  behavior in the infrared region of photon integration, although the complete fourth-order result is infrared convergent.<sup>16</sup> In the calculation presented in this paper, all traces, projections, and reduction to Feynman parametric integrals are done automatically by REDUCE, an algebraic computation program written by Hearn.<sup>19</sup> The definitions of the required subsidiary variables in terms of the Feynman parameters are obtained by alternate methods, the standard technique given in Ref. 15 and the method developed by Nakanishi and others.<sup>20</sup> The integrals over the Feynman parameters (up to five dimensions) are performed numerically (often to 0.1% precision) using a program originally written by Sheppey and modified by Dufner. In this method of multidimensional integration, more fully described in Ref. 21, one cal-

culates the usual Riemann sum, taking the central value of the integrand from an average over two random points within each hypercube. The difference of the function values is used to compute a variance and error for the integration; on successive iterations the computer readjusts the grid to minimize the variance. Many of the techniques used in this paper are similar to those by Aldins *et al.*<sup>21</sup> for the calculation of the photon-photon scattering contribution to the sixth-order electron and muon magnetic moments.

Our numerical result for the fourth-order slope is

$$m^2 \frac{\partial F_1^{(4)}}{\partial q^2} \Big|_{q^2=0} = \frac{\alpha^2}{\pi^2} [0.48 \pm 0.07] . \quad (2.5)$$

The contributions of the individual graphs are tabulated in Table III. The discrepancy with the results of Ref. 12 originates in an over-all sign disagreement and in the calculation of the constant terms in the crossed and corner graphs [see Figs. 1(a) and 1(b)]. In the case of the corner graph, this discrepancy is quite large. The revised theoretical values for the Lamb shifts in H, D, He<sup>+</sup>, and Li<sup>++</sup> are shown in Table I.

### III. VACUUM POLARIZATION AND FERMION SELF-ENERGY INSERTIONS

The contribution of the graph with the second-order vacuum polarization insertion [Fig. 1(c)] is easiest to calculate, and we start our discussion here. The effect of second-order vacuum polarization is summarized by a modification to the photon propagator,<sup>22</sup>

$$\frac{1}{k^2 - \lambda^2 + i\epsilon} \rightarrow \frac{1}{k^2 - \lambda^2 + i\epsilon} + \frac{\alpha}{\pi} \int_0^1 dz \frac{z^2 (1 - \frac{1}{3} z^2)}{1 - z^2} \times \frac{1}{k^2 - 4m^2/(1 - z^2) + i\epsilon} . \quad (3.1)$$

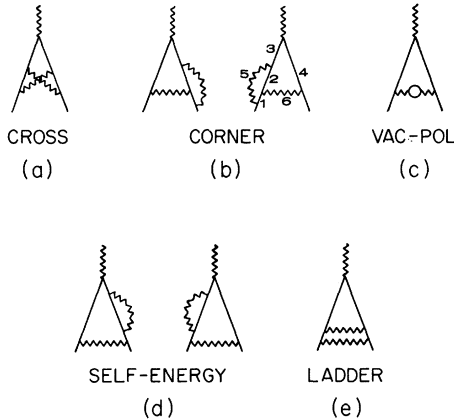


FIG. 1. Feynman diagrams for the fourth-order vertex of the electron required to compute the anomalous magnetic moment  $F_2(0)$  and the slope  $F_1'(0)$ .

TABLE III. Comparison of the results of this calculation and that of Ref. 12(a) for the Feynman graph contributions to  $a_4 = m^4 dF_1/dq^2(q^2=0)/(\alpha^2/\pi^2)$ .<sup>a</sup>

		Ref 12(a)	This calculation
$a_{\text{cross}}$	[Fig. 1(a)]	$\frac{13}{36} \ln \lambda^{-2}$ -2.314	$-\frac{13}{36} \ln \lambda^{-2}$ +2.37 ± 0.2
$a_{\text{corner}}$	[Fig. 1(b)]	$-\frac{1}{12} \ln^2 \lambda^{-2}$ $+\frac{1}{12} \ln \lambda^{-2}$ +2.432	$\frac{1}{12} \ln^2 \lambda^{-2}$ $-\frac{1}{12} \ln \lambda^{-2}$ -1.91 ± 0.02
$a_{\text{vacuum-polarization}}$	[Fig. 1(c)]	-0.0316	+0.0316 ± 0.0002
$a_{\text{self-energy}}$	[Fig. 1(d)]	$\frac{1}{12} \ln^2 \lambda^{-2}$ $-\frac{1}{12} \ln \lambda^{-2}$ -1.688	$-\frac{1}{12} \ln^2 \lambda^{-2}$ $+\frac{1}{12} \ln \lambda^{-2}$ +1.68 ± 0.01
$a_{\text{ladder}}$	[Fig. 1(e)]	$-\frac{13}{36} \ln \lambda^{-2}$ +1.710	$+\frac{13}{36} \ln \lambda^{-2}$ -1.69 ± 0.02
$a_4$		0.108	0.48 ± 0.07

<sup>a</sup>Corner and self-energy graph results include the contribution of mirror graphs. The infrared behavior is expressed in terms of a photon-mass parametrization for  $\lambda^2 \ll m^2$ . The infrared convergent ladder plus cross contributions (0.68 ± 0.04) as well as the corner plus self-energy contribution (-0.23 ± 0.03) could be obtained without knowledge of the infrared divergent behavior of the individual graphs, which were, however, found to be consistent with the negative of the asymptotic behavior ( $\lambda^2 \ll m^2$ ) given in Ref. 12. The individual noninfrared remainders given in the last column were determined from fits with the logarithmic terms constrained to those values plus "background" terms multiplying  $\sqrt{\lambda^2}$ ,  $\sqrt{\lambda^2} \ln \lambda^2$ , and  $\lambda^2 \ln \lambda^2$ .

Note that the second-order contribution to the slope of the Dirac form factor

$$m^2 \frac{\partial F_1^{(2)}}{\partial q^2} \Big|_{q^2=0} = \frac{\alpha}{\pi} \int_0^1 v dv \times \frac{\frac{2}{3} v^2 + 1 - v + \frac{1}{2} v^4 + (\lambda^2/m^2)(1-v)(1-v + \frac{1}{3} v^2)}{[v^2 + (\lambda^2/m^2)(1-v)]^2} . \quad (3.2)$$

is positive for all  $\lambda^2$ . Insertion of (3.1) is effectively a sum over various  $\lambda^2$  with a positive weight function. The vacuum polarization (VP) contribution to  $a_4$  is thus of the same sign as the second-order slope and hence gives a positive Lamb-shift contribution. (Thus, as is usual, the VP modification strengthens the contribution of one-photon exchange.) Upon numerical integration, we obtain

$$a_4(\text{VP}) = 0.0316 \pm 0.0002 , \quad (3.3)$$

in contrast to a negative Lamb-shift contribution of the same magnitude in Refs. 12 and 13.

The fermion self-energy correction [Fig. 1(d)] is accomplished by substituting

$$1/(p/-m + i\epsilon) \rightarrow \Sigma_f(p) \quad (3.4)$$

in each leg of the second-order vertex. Here  $\Sigma_f$  is

the twice-subtracted part of the self-energy insertion:

$$\Sigma(p) = A + (\not{p} - m)B + (\not{p} - m)^2 \Sigma_f(p), \quad (3.5)$$

$$\Sigma_f(p) = \frac{\alpha}{2\pi} \int_0^1 dx \int_0^1 dz \frac{\omega(x, z) [\not{p} + \not{\mathcal{M}}(x, z)]}{p^2 - r(x, z)m^2 + i\epsilon}, \quad (3.6)$$

where

$$\begin{aligned} \omega &= s(1-x)z, \\ r &= \frac{x(1-x)z + (\lambda^2/m^2)(1-x) + x^2}{x(1-x)z}, \\ \mathcal{M} &= \frac{m[s(1-x) - (1+x)]}{s(1-x)}, \\ s &= 1 - 2 \frac{z(1+x)x}{x^2 + (1-x)\lambda^2/m^2}. \end{aligned} \quad (3.7)$$

It should be emphasized that great care must be used in extracting  $\Sigma_f$  to keep all terms in  $\lambda^2$ .<sup>23</sup>

The method of calculation is similar to that for the graph with VP insertion. The second-order contributions to  $F_1'(0)$  with one fermion propagator replaced by

$$\not{p} + \not{\mathcal{M}}(x, z) / [p^2 - r(x, z)m^2 + i\epsilon]$$

is

$$\begin{aligned} m^2 \frac{\partial F_1^{(2)}(q^2, \mathcal{M}, r)}{\partial q^2} \Big|_{q^2=0} &= \frac{\alpha}{2\pi} \int_0^1 dz_1 dz_2 dz_3 \\ &\times \delta(1 - z_1 - z_2 - z_3) \\ &\times \left( \frac{z_2 z_3 + (1 - z_2)(1 - z_3)}{(1 - z_1)^2 + z_1(\lambda^2/m^2) + (r - 1)z_2} \right. \\ &\left. + \frac{[(\mathcal{M}/m) - 4z_1 + z_1^2] z_2 z_3}{[(1 - z_1)^2 + z_1(\lambda^2/m^2) + (r - 1)z_2]^2} \right). \end{aligned} \quad (3.8)$$

Then  $\partial F^{(4d)}/\partial q^2|_{q^2=0}$  is given by

$$\begin{aligned} m^2 \frac{\partial F^{(4d)}}{\partial q^2} \Big|_{q^2=0} &= \frac{\alpha}{\pi} \int_0^1 dx \int_0^1 dz \\ &\times \omega(x, z) \frac{\partial F_1^{(2)}(q^2, \mathcal{M}, r)}{\partial q^2} \Big|_{q^2=0}, \end{aligned} \quad (3.9)$$

where a factor of 2 is included for the mirror graph. This integral is easily carried out numerically for various  $\lambda^2$  and can be compared as  $\lambda^2 \rightarrow 0$  with the analytic result of WBK<sup>12</sup> and Soto,<sup>13</sup>

$$\begin{aligned} m^2 \frac{\partial F^{(4d)}}{\partial q^2} \Big|_{q^2=0, \lambda \ll m} &= \frac{1}{12} \ln^2(m^2/\lambda^2) - \frac{1}{72} \ln(m^2/\lambda^2) - 1.688 \dots \end{aligned} \quad (3.10)$$

The result for our calculations is shown in Fig. 2,

and we see that, apart from an over-all sign, excellent agreement is obtained.

The common feature that the actual dependence of the integrals pulls appreciably away from the asymptotic formula even at  $\lambda^2$  as small as  $10^{-3} m^2$  reflects the fact that Eq. (3.9) is a negative function of  $\lambda^2$  for all positive  $\lambda^2$  and does not cross the axis as do the extrapolated asymptotic formulas.

#### IV. CORNER GRAPH

In calculating the contributions from the graphs with vacuum polarization and fermion self-energy insertions, we followed the procedure of first calculating the renormalized amplitudes for the subgraphs, inserting their spectral integral representations into the second-order vertex graphs, and then doing the over-all renormalization subtractions.

It is also possible to use a similar procedure<sup>12</sup> for the corner graph of Figure 1(b) (and the ladder graph to be treated in Sec. V). However, the integral representation for the renormalized vertex subgraph is much more complicated than that for self-energy graphs, requiring, in general, a dispersion representation in the three off-shell variables. We have used instead a different approach, which is simpler, at least when the computer is

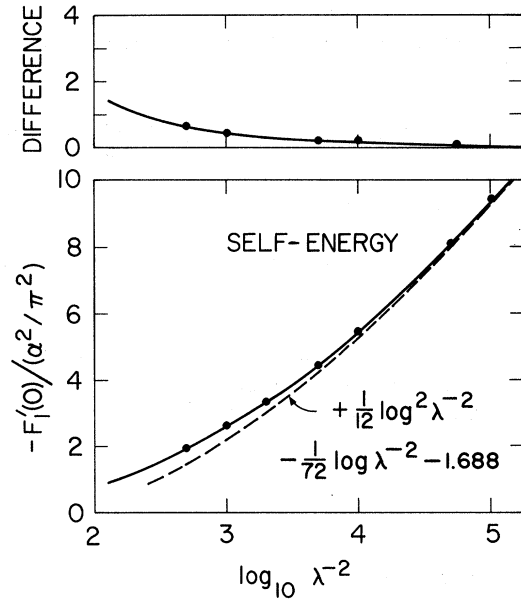


FIG. 2. Contribution to the slope of the Dirac form factor in fourth order from fermion self-energy insertions in the second-order vertex [Fig. 1 (d)]. The solid curve is the result of numerical calculation for various  $\lambda^2$  (in units of the electron mass squared). The results of this calculation agree asymptotically with Soto's analytic result of  $\lambda \rightarrow 0$  (dashed curve) except for over-all sign. The top graph gives the difference between the two curves. The error bars represent approximately  $1\sigma$  in the numerical integration.

used for the algebraic reduction and numerical evaluation of the integrals. It will be helpful to first outline the method and then present it in detail. We first combine all the denominators of the unrenormalized amplitudes and project out the Dirac form factor  $F_1$ . The internal momentum integrations are then done and the result is expressed as a five-dimensional integration over parameters. The ultraviolet divergences corresponding to the vertex subgraph and to the graph as a whole will, of course, still be present in the parametric integral. The subtraction necessary to remove the internal logarithmic divergence is accomplished by recomputing this expression with the vertex subgraph computed with the external momenta which flow through it constrained to the mass shell, again combining all six denominators first. The integrands are then subtracted and the resulting five-dimensional integral will contain only the over-all divergence, which is subtracted automatically at  $q^2 = 0$ , when we compute  $F_1'(0)$ . Once the difference of integrands is differentiated with respect to  $q^2$ , and  $q^2$  is set equal to 0, the result (for  $\lambda^2 > 0$ ) is a convergent five-dimensional integral for  $F_1'(0)$ , which we can evaluate numerically by computer. We shall describe several checks on the calculations of  $F_1'(0)$ , including the evaluation of corner- and crossed-graph contributions to  $F_2(0)$ .

The unrenormalized amplitude for the corner graph is

$$\begin{aligned} M_{\text{corner}}^\nu &= 2(-ie)^5 i^4 (-i)^2 \int \frac{d^4 l_1}{(2\pi)^4} \frac{d^4 l_2}{(2\pi)^4} \left[ 1 / \prod_{i=1}^6 (p_i^2 - m_i^2) \right] \\ &\quad \times \bar{u}(p + \frac{1}{2}q) [\gamma_\beta (\not{p}_4 + m) \\ &\quad \times \gamma^\nu (\not{p}_3 + m) \gamma_\alpha (\not{p}_2 + m) \gamma^\beta (\not{p}_1 + m) \gamma^\alpha] u(p - \frac{1}{2}q) \\ &= -ie \bar{u}(p + \frac{1}{2}q) J_{\text{corner}}^\nu u(p - \frac{1}{2}q) . \end{aligned} \quad (4.1)$$

The factor of 2 is included for the mirror graph.

We can automatically determine the contribution to the form factors [see Eq. (2.1)] through

$$F_j(q^2) = \frac{1}{4} \text{Tr} \left[ (\not{p} + \frac{1}{2}\not{q} + m) J^\mu (\not{p} - \frac{1}{2}\not{q} + m) \Lambda_\mu^{(j)} \right], \quad (4.2)$$

where<sup>24</sup>

$$\Lambda_\mu^{(1)} = [3m \not{p}_\mu - \not{p}^2 \gamma_\mu] 4p^{-4}, \quad (4.3)$$

$$\Lambda_\mu^{(2)} = [m^2 \not{p}^2 \gamma_\mu - m(m^2 + \frac{1}{2}q^2) \not{p}_\mu] q^{-2} p^{-4}, \quad (4.4)$$

with

$$\not{p}^2 = m^2 - \frac{1}{4}q^2, \quad \not{p} \cdot q = 0. \quad (4.5)$$

After the traces and index contractions are performed to obtain  $F_1(q^2)$ , we have to consider integrals of the form

$$I = \int \left( d^4 l_1 d^4 l_2 / \prod_{i=1}^6 (p_i^2 - m_i^2 + i\epsilon) \right) F(p_j), \quad (4.6)$$

where  $m_i$  is the mass corresponding to line  $i$  and

$$p_j = k_j + \sum_{r=1}^2 \eta_{jr} l_r \quad (j = 1, \dots, 6). \quad (4.7)$$

Here  $\eta_{jr}$  is the projection ( $\pm 1, 0$ ) of  $p_j$  along  $l_r$ , and  $k_j$  can be any choice of fixed momenta (independent of  $l_r$ , proportional to  $p, q$ ) such that four-momentum is retained at the five vertices. Feynman parameters are now introduced:

$$\begin{aligned} \left( \prod_{j=1}^6 (p_j^2 - m_j^2 + i\epsilon) \right)^{-1} &= 5! \int dz_1 \dots dz_6 \delta \left( 1 - \sum_{i=1}^6 z_i \right) / \\ &\quad \left( \sum_j z_j (p_j^2 - m_j^2 + i\epsilon) \right)^6. \end{aligned} \quad (4.8)$$

If we choose the  $k_j$  such that<sup>15</sup>

$$\sum_{j=1}^6 z_j k_j \eta_{jr} = 0 \quad (r = 1, 2), \quad (4.9)$$

then the  $k_j \cdot l_r$  cross terms in the denominator vanish. For convenience we define

$$U = \det U_{rr'}, \quad U_{rr'} = \sum_{j=1}^6 z_j \eta_{jr} \eta_{jr'}, \quad (4.10)$$

$$D = \sum_{j=1}^6 z_j (m_j^2 - k_j^2). \quad (4.11)$$

The basic integration over loop moment  $q$  then gives

$$5! \int d^4 l_1 d^4 l_2 / [-D + \sum_{rr'} U_{rr'} l_r \cdot l_{r'} + i\epsilon]^6 = i^2 \pi^4 / D^2 U^2. \quad (4.12)$$

The numerator also contains terms quadratic and quartic in the loop momentum four-vectors. For the  $l_a \cdot l_b$  terms<sup>21</sup> we replace

$$l_a \cdot l_b \rightarrow -2B_{ab}(D/U), \quad (4.13)$$

where  $B_{ab}$  is the signed cofactor of  $U_{ab}$  in  $U$ . Also, we have

$$\begin{aligned} l_a \cdot l_b l_c \cdot l_d \rightarrow [4B_{ab}B_{cd} + B_{ad}B_{bc} + B_{ac}B_{bd}] (D^2/U^2) \\ \times [\ln(\Lambda^2/D) + 1]. \end{aligned} \quad (4.14)$$

The dependence on the ultraviolet cutoff  $\Lambda^2$  is eliminated because of the over-all subtraction at  $q^2 = 0$ , and we can in fact replace

$$1 + \ln[\Lambda^2/D(q^2)] - \ln[D(q^2=0)/D(q^2)]. \quad (4.15)$$

These substitutions can also be readily done by REDUCE,<sup>19</sup> yielding the reduction of the matrix element to an integrand for parametric integration (in the form of a punched deck in FORTRAN form).<sup>25</sup>

As an alternate method to the above and as a check we have also used the graphical method of reduction to parametric form developed by Nakanishi<sup>20</sup> and others. A particularly valuable check is obtained for the quantity

$$U \sum_{j=1}^6 z_j k_j^2 = W_p m^2 + W_q q^2, \quad (4.16)$$

in which the parametric functions  $W_p$  and  $W_q$  can be read off very simply from the Feynman graph structure.

The internal vertex renormalization subtraction must yet be performed. Thus we subtract from  $M_{\text{corner}}^\nu$  the corresponding amplitude with the *internal* loop calculated as if lines 3 and 6 [see Fig. 1(b)] were on their respective mass shell:

$$\begin{aligned} M_{\text{corner sub}}^\nu &= 2(-ie)^5 i^4 (-i)^2 \\ &\times \int \frac{d^4 l_1}{(2\pi)^4} \bar{u} \gamma_\alpha (\not{p}_4 + m) \gamma^\nu (\not{p}_3 + m) \gamma^\alpha u \\ &\quad \prod_{j=3,4,6} (\not{p}_j^2 - m_j^2) \\ &\times \int \frac{d^4 l_2}{(2\pi)^4} \frac{\frac{1}{4} \text{Tr}[\gamma_B (\not{p}_2 + m) \not{K} (\not{p}_1 + m) \gamma^B (\not{K} + m)]}{m^2 \prod_{j=1,2,5} (\not{p}_j^2 - m_j^2)}, \end{aligned} \quad (4.17)$$

where

$$p_1 + p_5 = p_2 + p_5 = R \quad \text{and} \quad R^2 = m^2. \quad (4.18)$$

This integrand is then subtracted from the above before numerical evaluation of the five-dimensional

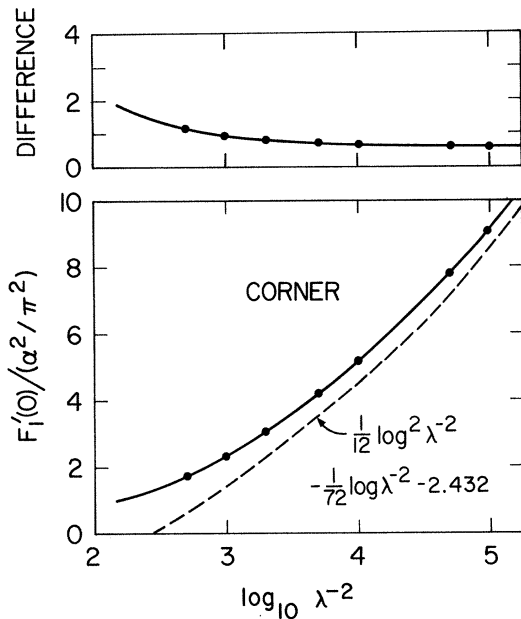


FIG. 3. Numerical results for the corner-graph contribution to  $F_1'(0)$  as a function of photon mass  $\lambda$ . The dashed curve is the negative of Soto's analytic result for the asymptotic region  $\lambda \rightarrow 0$ . The top graph indicates that the two curves become parallel in the asymptotic region rather than joining. This is the major source of numerical discrepancy between the results of the two calculations.

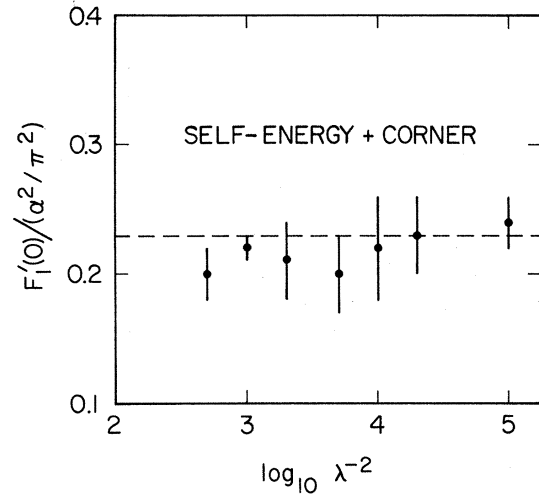


FIG. 4. Sum of corner plus self-energy contributions [Figs. 1(b) and 1(d)] to  $F_1'(0)$  in fourth order as a function of photon mass  $\lambda^2$ . The expectation that this sum of contributions [Figs. 1(b) and 1(d)] is finite in the infrared is confirmed. The contribution  $(-0.23 \pm 0.03) (\alpha/\pi)^2$  can be obtained without any knowledge of the infrared divergent behavior of the individual contributions.

integral.<sup>25</sup> The subtraction is sufficient to remove the ultraviolet divergence associated with the vertex subgraph which appears as logarithmic singularity as  $z_1, z_2, z_5 \rightarrow 0$ . The over-all divergence, characterized by the  $\Lambda^2$  in Eq. (4.14), is removed automatically when we compute  $F_1'(0)$ . Thus, an ultraviolet cutoff is unnecessary and the integral can be performed as a function of  $m_5^2 = m_6^2 = \lambda^2$ .

Our result for the contribution to  $F_1'(0)$  from the corner graph along with the analytic result for the asymptotic region ( $\lambda \ll m$ ) given by Soto is shown in Fig. 3. After correcting for the sign discrepancy the two curves become parallel in the asymptotic ( $\lambda \rightarrow 0$ ) region rather than joining. The expectation that the sum of corner plus self-energy contributions are finite for  $\lambda \rightarrow 0$  is confirmed in Fig. 4.

In order to determine the constant term in the corner-graph contribution, we have constrained the coefficients of the  $\ln \lambda^{-2}$  and  $\ln \lambda^{-2}$  terms to be the negative of Soto's and have performed several types of least-square fits to the results of the numerical integration using "background" terms multiplying  $\sqrt{\lambda^2}$ ,  $\sqrt{\lambda^2} \ln \lambda^2 \ln \lambda^2$ . The resulting constant term from the corner graph, shown in Fig. 1, column 2, differs substantially from the constant term in Soto's expression. A consistent value for the sum of self-energy and corner contributions for  $\lambda^2 \rightarrow 0$  can be obtained directly from Fig. 4 without any detailed curve fitting or knowledge of the infrared divergent behavior of the individual contributions.

As another check on the calculation, we have also

calculated the corner-graph contribution using *intermediate renormalization*. In this method the subtraction term is computed as in Eq. (4.17), but the internal vertex is computed with its fermion and photon legs all on the  $m=0$  mass shell. The subtraction term can be obtained immediately from the unrenormalized amplitude by replacing  $k_1, k_2 \rightarrow 0$ ,  $B_{14} \rightarrow 0$ , and keeping only the terms in  $U, D, k_3$ , and  $k_4$  which are of lowest order in  $z_1, z_2$ , or  $z_5$ . A complete discussion of intermediate renormalization in Feynman parameter space is given in Ref. 26.

The correction term which compensates for the error made in renormalizing at  $m=0$  is simply

$$(2)dF_1^2/dq^2|_0 \times [\Lambda^{(2)}(0, 0, 0) - \Lambda^{(2)}(m, m, 0)] \quad (4.19)$$

where the first factor is defined in Eq. (3.2) and where

$$\begin{aligned} \Lambda^{(2)}(0, 0, 0) - \Lambda^{(2)}(m, m, 0) &= \frac{\alpha}{2\pi} \int_0^1 dz \\ &\times z \left( \frac{1}{z + (\lambda^2/m^2)(1-z)} - \frac{(-2+2z+z^2)}{z^2 + (\lambda^2/m^2)(1-z)} \right. \\ &\left. + \ln \frac{z^2 + (\lambda^2/m^2)(1-z)}{z + (\lambda^2/m^2)(1-z)} \right) \\ &\xrightarrow{\lambda \ll m} \frac{\alpha}{\pi} \left[ \ln \left( \frac{m}{\lambda} \right) - \frac{7}{8} \right] \end{aligned} \quad (4.20)$$

is calculated from the coefficient of  $\gamma_\alpha$  of the unrenormalized vertex in second order. The numerical results are consistent with that obtained using re-

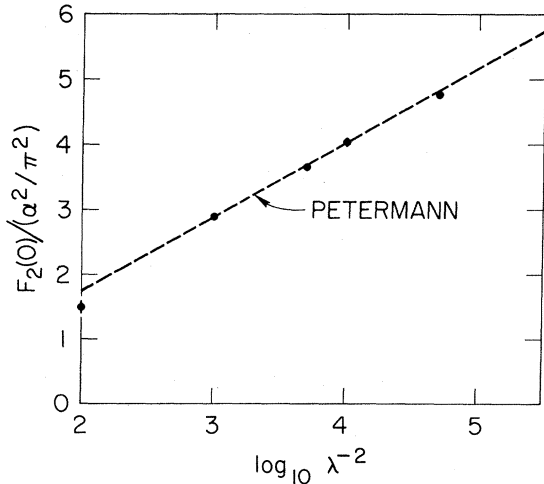


FIG. 5. Numerical contribution to the fourth-order magnetic moment of the electron from the corner diagram [Fig. 1(b)] as a function of photon mass. The dashed line is Petermann's result (Ref. 18),  $F_2^{1b}(0) = [\frac{1}{2} \ln \lambda^{-2} - 0.564] (\alpha^2/\pi^2)$  derived from  $\lambda \rightarrow 0$ . As in the case for  $F_1'(0)$ , the infrared divergence is cancelled by the self-energy contribution [Fig. 1(d)].

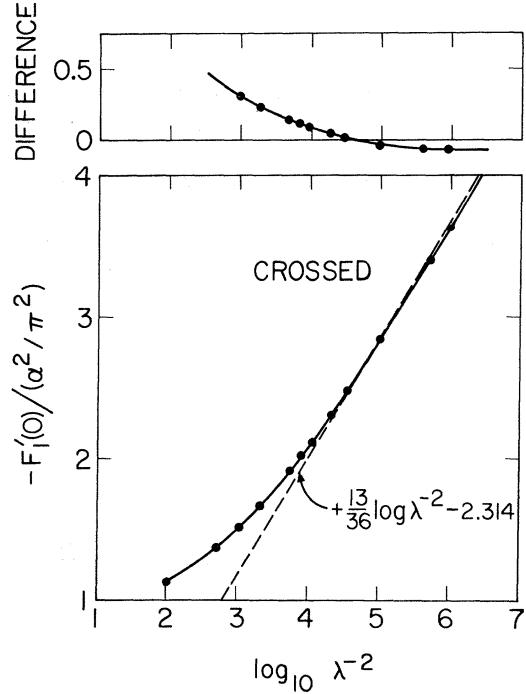


FIG. 6. Numerical contribution to  $F_1'(0)$  from the crossed diagram [Fig. 1(a)] as a function of photon mass  $\lambda$ . The dashed curve is the negative of Soto's analytic result for  $\lambda \rightarrow 0$ . The top graph shows that the two curves become parallel in the asymptotic region, disagreeing slightly in the value of the noninfrared remainder.

normalization on the mass shell.

As a final check on the corner-graph contribution to  $F_1'(0)$  we have also projected out the contribution of this graph to  $F_2(0)$ , the anomalous magnetic moment of the electron. Since the same parametric functions that enter  $F_1$  also enter  $F_2$  (since the same method of internal renormalization is used) and since the same integration program is used, this is a reasonably good check on the calculation. The result shown in Fig. 5 is in excellent agreement with Petermann's result.<sup>18</sup> The logarithmic dependence on the photon mass, which cancels when the contributions of all fourth-order graphs to  $F_2(0)$  are added, arises from the integration region  $z_1, z_2 \sim 0$ . The choice of variables

$$\begin{aligned} z_1 &= vu, \quad z_2 = v(1-u), \\ dz_1 dz_2 &= v dv du \quad (0 < u < 1) \end{aligned} \quad (4.21)$$

improves the integration efficiency, since there is slow dependence of the integrand on  $u$ . Similar variable changes were made in all of the numerical calculations in order to check consistency and improve the integration efficiency.

#### V. LADDER AND CROSSED-LADDER GRAPHS

The two remaining contributions to the slope of

the Dirac form factor in fourth order are shown in Figs. 1(a) and 1(e). The sum of the ladder and crossed-ladder contributions is infrared convergent and it is convenient to discuss them together.

The calculation of the crossed-ladder contribution is quite easy, since there is no internal ultraviolet divergence. The method of Sec. IV can again be used, except that for this graph, no internal renormalization subtraction need be made. The result is shown in Fig. 6 and again, apart from an over-all sign, agreement is found with the  $\ln \lambda^{-2}$  term in Soto's expression. However, as shown in Fig. 1, we disagree slightly with Soto in the finite (non-infrared) term. We have also calculated the contribution of this graph to  $F_2(0)$  and have again found excellent agreement with Petermann's result.

The calculation of the ladder-graph contribution is nearly identical to that of the corner graph. The internal vertex subtraction is carried out in the same way, and in this case we find complete agree-

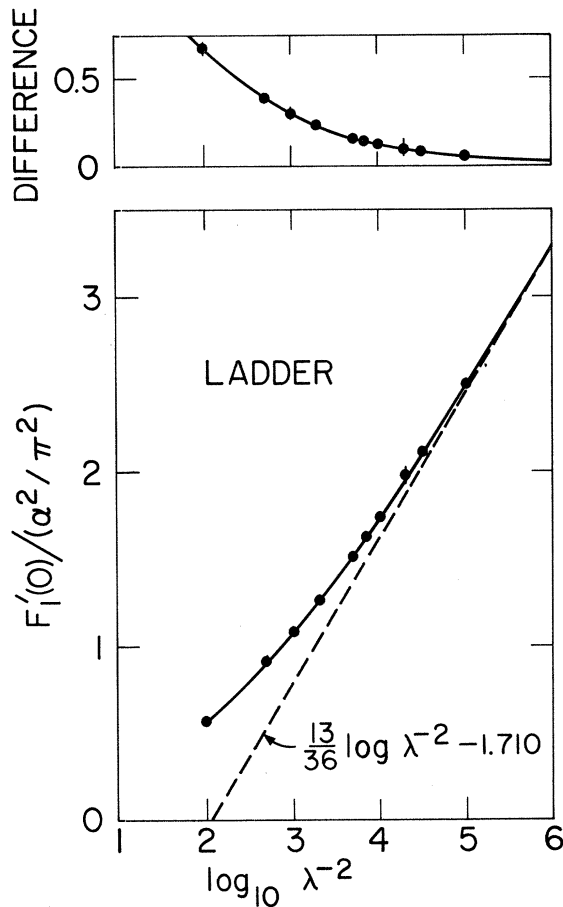


FIG. 7. Numerical contribution to  $F'_1(0)$  from the ladder diagram [Fig. 1(e)] as a function of photon mass  $\lambda$ . The dashed curve is the negative of Soto's analytic result for the asymptotic region  $\lambda \rightarrow 0$ . Within errors, the two curves are in good agreement as  $\lambda \rightarrow 0$ .

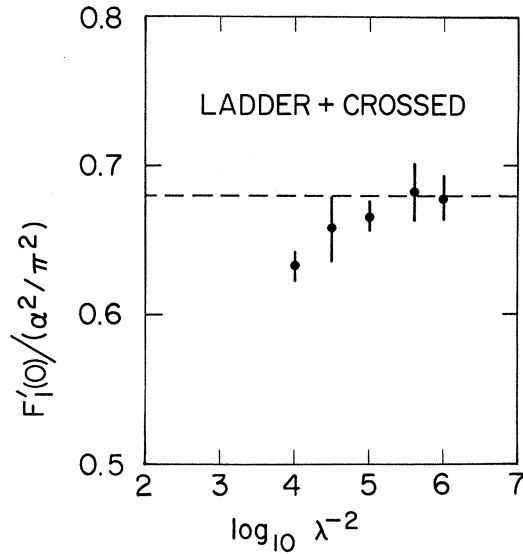


FIG. 8. Sum of ladder plus crossed diagram [Figs. 1(a) and 1(d)] contributions to  $F'_1(0)$  as a function of photon mass  $\lambda^{-2}$ . The combined contribution  $(0.68 \pm 0.4) (\alpha/\pi)^2$  to Eq. (2.5) can be obtained without any knowledge of the infrared divergent behavior of the individual contributions.

ment with (the negative of) Soto's result. The comparison is shown in Fig. 7. The sum of ladder plus crossed-graph contributions is shown in Fig. 8.

## VI. CONCLUSION

The total contribution to the slope of the Dirac form factor in fourth order is given in Eq. (2.5). The corresponding contribution to the  $nS_{1/2}-nP_{1/2}$  level splitting is  $(0.45 \pm 0.07 \text{ MHz}) \times [Z^4(2/n)^3]$ , an increase of  $(0.35 \pm 0.07 \text{ MHz}) \times [Z^4(2/n)^3]$  over the previous contributions.<sup>2,3,6</sup> Our result for the fourth-order corner graph, which is the primary source of the revision, has been confirmed by a new partially analytic and partially numeric calculation by de Rafael, Lautrup, and Petermann, and by a completely analytic calculation of Barbieri, Mig-naco, and Remiddi.<sup>27</sup> It would be desirable, however, to have a completely analytic calculation of the entire  $F'_1$  contribution in order to eliminate the error limits introduced by the numerical calculations. A complete calculation of the order- $\alpha(Z\alpha)^6$  contribution to the Lamb shift will also be required in order to obtain a theoretical prediction with a limit of error several times smaller than the errors quoted for the experimental results.

The reconciliation of the QED calculations with the Lamb-shift experiments (see Table I) is very gratifying. At the present time, not one of the sensitive QED comparisons of theory and experiment is in serious disagreement.<sup>3</sup>

Unlike the colliding-beam,  $(g-2)_\mu$ , and hyper-fine-splitting measurements, the Lamb-shift mea-

surements are not particularly useful for limiting high-momentum transfer modifications of QED,<sup>28</sup> although the current agreement with experiment does rule out speculations of the type discussed by Barrett *et al.*<sup>29</sup> (long charge tails on the nucleus) and Yennie and Farley<sup>30</sup> (low-mass scalar particle exchange). It is interesting to note that the magnitude and  $Z$  and  $n$  dependence of the proposed modifications of the hadronic contribution to the Lamb shift are the same as those caused by the reevaluation of the fourth-order contributions discussed in this paper.

## ACKNOWLEDGMENTS

We wish to thank our colleagues at SLAC especially S. Drell and J. Primack, for their encouragement and helpful discussions. We also wish to thank Professor D. R. Yennie for several stimulating discussions and helpful suggestions. The cooperation of the SLAC Computation Center is also deeply appreciated. We also acknowledge our great debt to A. C. Hearn for making his algebraic computation program REDUCE available to us, and to G. Sheppey for the development of his numerical integration program.

\*Work supported by the U. S. AEC.

†Present address: Department of Physics, Harvard University, Cambridge, Mass. 02138.

<sup>1</sup>(a) W. E. Lamb, Jr. and R. E. Retherford, *Phys. Rev.* **86**, 1014 (1952); and references therein; (b) S. Triebwasser, E. S. Dayhoff and W. E. Lamb, Jr., *ibid.* **89**, 98 (1953); **89**, 106 (1953).

<sup>2</sup>H. A. Bethe, *Phys. Rev.* **72**, 339 (1947).

<sup>3</sup>S. J. Brodsky, in 1969 International Symposium on Electron and Photon Interactions at High Energies, Liverpool, England, 1969, SLAC-PUB-676 (unpublished).

<sup>4</sup>(a) R. T. Robiscoe and T. W. Shyn (unpublished); (b) see B. Taylor, W. Parker, and D. Langenberg, *Rev. Mod. Phys.* **41**, 375 (1969); (c) B. L. Cosens, *Phys. Rev.* **173**, 49 (1968).

<sup>5</sup>See Refs. for Table I.

<sup>6</sup>(a) S. L. Kaufman, W. E. Lamb, K. R. Lea, and M. Leventhal, *Phys. Rev. Letters* **22**, 507 (1969); (b) T. W. Shyn, W. L. Williams, R. T. Robiscoe, and T. Rebane, *ibid.* **22**, 1273 (1969); (c) T. V. Vorburger and B. L. Cosens, *ibid.* **23**, 1273 (1969).

<sup>7</sup>A. J. Layzer, *Phys. Rev. Letters* **4**, 580 (1960).

<sup>8</sup>R. Karplus, A. Klein, and J. Schwinger, *Phys. Rev.* **86**, 288 (1952).

<sup>9</sup>G. W. Erickson and D. R. Yennie, *Ann. Phys. (N.Y.)* **35**, 271 (1965); **35**, 447 (1965).

<sup>10</sup>E. E. Salpeter, *Phys. Rev.* **87**, 328 (1952).

<sup>11</sup>H. Grotch and D. R. Yennie, *Rev. Mod. Phys.* **41**, 350 (1969).

<sup>12</sup>(a) S. J. Weneser, R. Bersohn, and N. Kroll, *Phys. Rev.* **91**, 1257 (1953); (b) M. F. Soto, Jr., *Phys. Rev. Letters* **17**, 1153 (1966), which is the only analytic calculation of the fourth-order contribution. It was previously estimated by Weneser, Bersohn, and Kroll (this reference).

<sup>13</sup>T. Appelquist and S. J. Brodsky, *Phys. Rev. Letters* **24**, 562 (1970).

<sup>14</sup>R. Mills and N. Kroll, *Phys. Rev.* **98**, 1489 (1955).

<sup>15</sup>We use the notation and conventions of J. D. Bjorken and S. D. Drell, *Relativistic Quantum Mechanics* (McGraw-Hill, New York, 1964). Note that a form factor which falls for spacelike  $q^2$  [ $dF_1(0)/dq^2 > 0$ ] reduces the binding of  $s$  states and therefore contributes a positive contribution to the Lamb shift. A derivation of Eq. (2.2) can be found in D. R. Yennie and G. W. Erickson, Ref. 9.

<sup>16</sup>It can be seen quite easily that the slope of the Dirac form factor in order  $\alpha^2$  will be convergent in the infrared by using the well-known result of Yennie, Frautschi, and Suura [*Ann. Phys. (N.Y.)* **13**, 379 (1961)] that the logarithmic dependence on the photon mass can be regrouped into a multiplicative exponential factor. A care-

ful analysis shows that the renormalized vertex  $\tilde{\Gamma}_\mu(p, p')$  can be written in the form

$$\begin{aligned} \tilde{\Gamma}_\mu(p, p') &= e^B \Gamma_\mu \text{NIR} \\ &= \gamma_\mu + B\gamma_\mu + \Lambda_\mu^{(2)} + \frac{1}{2}(B)^2\gamma + B\Lambda_\mu^{(2)} + \Lambda_\mu^{(4)} + O(\alpha^3), \end{aligned}$$

where  $B$  contains all the logarithmic dependence on the photon mass and  $\Lambda_\mu^{(2)}$  and  $\Lambda_\mu^{(4)}$  are finite when the photon mass is set equal to 0. Since both  $B$  and the  $F_1$  part of  $\Lambda_\mu^{(n)}$  vanish like  $q^2$  when  $q^2 \rightarrow 0$ , we see that the fourth-order Dirac form factor to order  $q^2$  is convergent in the infrared. We wish to thank D. R. Yennie for discussions on this point. It must also be shown that the photon mass device leads to the same noninfrared remainder as the actual regularization procedure from binding corrections. This is in fact what has been established by Mills and Kroll, Ref. 14.

<sup>17</sup>R. Karplus and N. M. Kroll, *Phys. Rev.* **77**, 536 (1950).

<sup>18</sup>A. Petermann, *Helv. Phys. Acta* **30**, 407 (1957).

<sup>19</sup>A. C. Hearn, Stanford University Report No. ITP-247, Stanford, Calif., 1968.

<sup>20</sup>N. Nakanishi, *Progr. Theoret. Phys. (Kyoto) Suppl.* **18**, 1 (1961); N. Nambu, *Nuovo Cimento* **6**, 1064 (1957); K. Symanzik, *Progr. Theoret. Phys. Kyoto* **20**, 690 (1958).

<sup>21</sup>J. Aldins, S. J. Brodsky, A. J. Dufner, and T. Kinoshita, *Phys. Rev. Letters* **23**, 441 (1969); and (to be published).

<sup>22</sup>This is simply the spectral representation for the photon propagator to first order in  $\alpha$ ; G. Källén, *Helv. Phys. Acta* **25**, 417 (1952).

<sup>23</sup>J. M. Jauch and F. Rohrlich, *The Theory of Photons and Electrons* (Addison-Wesley, Reading, Mass., 1955). The result for  $\lambda^2=0$  in Eqs. (9)–(24), which is infrared divergent, contains a sign error in one term. The subtraction constant  $B$ , which contributes to electron wave function renormalization, is also infrared divergent in the limit  $\lambda^2 \rightarrow 0$ . It is, of course, exactly cancelled due to the Ward identity, once vertex and external line wave function renormalization constants are included.

<sup>24</sup>S. J. Brodsky and J. D. Sullivan, *Phys. Rev.* **156**, 1644 (1967).

<sup>25</sup>The programs for doing the algebraic reduction and numerical integration are available in SLAC-PUB-756. The numerical integration program contains the definitions of all subsidiary quantities  $k_j$ ,  $W_p$ ,  $W_q$ ,  $U$ , in terms of  $z_1 \dots z_6$ .

<sup>26</sup>T. Appelquist, *Ann. Phys. (N.Y.)* **54**, 27 (1969).

<sup>27</sup>E. deRafael, B. Lautrup, and A. Petermann, Th-

1140-CERN (unpublished); R. Barbieri, J. A. Mignaco, and E. Remiddi, University of Pisa Report, 1970 (unpublished).

<sup>28</sup>J. Kraus, Nucl. Phys. B11, 588 (1969).

<sup>29</sup>R. C. Barrett, S. J. Brodsky, G. W. Erickson, and

M. M. Goldhaber, Phys. Rev. 166, 1587 (1968).

<sup>30</sup>See D. R. Yennie, in Proceedings of the International Symposium on Electron and Photon Interactions at High Energies, SLAC, Stanford, Calif., 1967 (unpublished).